AD-A049 352 MICHIGAN UNIV ANN ARBOR ELECTRON PHYSICS LAB F/G 9/5
FUNDAMENTAL OPERATING CHARACTERISTICS OF PULSED TRAPATT DIODE O--ETC(U)
OCT 77 N A MASNARI, J R EAST, D G SWANSON DAAG39-76-C-0080
UNCLASSIFIED 014516-F NL

| OF |
ADA049352

END
DATE FILMED
3-78
DDC

Prepared by

Electron Physics Laboratory
University of Michigan
Ann Arbor, MI 48109

Under Contract

DAAG39-76-C-0080

U.S. Army Mate
and Readiness
HARRY DIAM
Adelphi, Maryl

N. A. Masnari, J. F. Earl, R. O. Sims

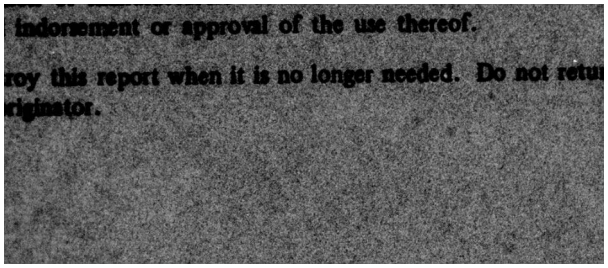
indorsement or approval of the use thereof.
roy this report when it is no longer needed. Do not retu
riginator.

UNCLASSIFIED

SECURITY CLASSIFICATION OF THIS PAGE *(When Data Entered)*

REPORT DOCUMENTATION PAGE

READ INSTRUCTIONS BEFORE COMPLETING FORM

1. REPORT NUMBER: Final - 1 (9) Final rept. 5 apr 76-31 May 77

2. GOVT ACCESSION NO.

3. RECIPIENT'S CATALOG NUMBER

4. TITLE *(and Subtitle)* (6)

FUNDAMENTAL OPERATING CHARACTERISTICS OF PULSED TRAPATT DIODE OSCILLATORS.

5. TYPE OF REPORT & PERIOD COVERED: Final Report, April 5, 1976-May 31, 1977

6. PERFORMING ORG. REPORT NUMBER (14): Ø14516-F

7. AUTHOR(a) (10): N. A. Masnari, J. R. East, and D. G. Swanson

8. CONTRACT OR GRANT NUMBER(a) (15): DAAG39-76-C-0080 new

9. PERFORMING ORGANIZATION NAME AND ADDRESS
Electron Physics Laboratory
University of Michigan
Ann Arbor, MI 48109

10. PROGRAM ELEMENT, PROJECT, TASK AREA & WORK UNIT NUMBERS
Program Element: 62616A
HDL Project: A77716

11. CONTROLLING OFFICE NAME AND ADDRESS
U.S. Army Materiel Development & Readiness Command
Alexandria, VA 22333

12. REPORT DATE (11): October 1977

13. NUMBER OF PAGES: 38

14. MONITORING AGENCY NAME & ADDRESS *(if different from Controlling Office)*
Harry Diamond Laboratory
2800 Powder Mill Road
Adelphi, MD 20783
(12) 39 p.

15. SECURITY CLASS. *(of this report)*: UNCLASSIFIED

15a. DECLASSIFICATION/DOWNGRADING SCHEDULE

16. DISTRIBUTION STATEMENT *(of this Report)*

Approved for public release; distribution unlimited.

DDC RECEIVED FEB 1 1978 B

17. DISTRIBUTION STATEMENT *(of the abstract entered in Block 20, if different from Report)*

18. SUPPLEMENTARY NOTES

DRCMS Code: 662616.H770011
DA-IL662616AH77
(16)

19. KEY WORDS *(Continue on reverse side if necessary and identify by block number)*

Avalanche Diode	Transient Behavior	Risetime Effects
TRAPATT Diode	TRAPATT Triggering Mechanisms	High Pulse Power TRAPATT Oscillators
Experimental Waveforms	IMPATT Oscillation	
Circuit Evaluation	Relaxation Oscillation	
Diode-Circuit Interaction	Bias Circuit Effects	UHF and S-Band Diodes

20. ABSTRACT *(Continue on reverse side if necessary and identify by block number)*

The objectives of the program are to investigate the TRAPATT turn-on mechanisms and to evaluate the effects of bias circuit and RF circuit configurations on the TRAPATT performance. A UHF TRAPATT oscillator has been investigated theoretically and experimentally to understand the device operation and the effect of the lumped circuit design on its performance. A computer program was developed to evaluate the effects of the finite transmission lines which interconnect the various lumped elements. The results indicate that the TRAPATT →

DD FORM 1 JAN 73 1473 EDITION OF 1 NOV 65 IS OBSOLETE

125 900

UNCLASSIFIED

SECURITY CLASSIFICATION OF THIS PAGE *(When Data Entered)*

20. turn-on mechanism depends both on the bias pulse rise time and the circuit design. An experimental probe was designed to allow the transient wave shapes to be recorded at the diode as well as at other points along the circuit. RF power was detected in the vicinity of the diode up through the 13th harmonic of the fundamental TRAPATT frequency.

Similar measurements were carried out for several S-band TRAPATT diodes in a coaxial circuit structure. The probes for the S-band structure were modified in an attempt to achieve better current and voltage waveshape information.

TABLE OF CONTENTS

ILLUSTRATIONS

ILLUSTRATIONS (cont'd)

1. Introduction

The objective of this program was to develop a better understanding of the operation of pulsed TRAPATT diode oscillators that eventually will lead to the formulation of design parameters for TRAPATT diode circuits. The investigations have been concerned with a variety of problems including the mechanisms of turn-on, the jitter of the pulse during turn-on, interactions of the device and the circuit, interaction of various frequencies within the device to produce mixing products and circuit requirements for efficient device operation. During the program the turn-on conditions of the UHF TRAPATT oscillator were studied and compared with earlier work carried out at S-band frequencies.[1] In that earlier work it was observed experimentally that TRAPATT operation invariably is accompanied by various other frequencies including bias circuit oscillations, VHF oscillations, IMPATT frequencies and related harmonic and subharmonic signals. The VHF oscillations were found to be responsible for the TRAPATT initiation if the bias-circuit pulse rise time was sufficiently fast. However, for slower bias-pulse rise times the IMPATT mode was observed to be responsible for launching the TRAPATT oscillation. In particular, the TRAPATT mode was observed to occur more rapidly, whenever the bias pulse had an extremely fast rise time and appreciable overshoot.

---

[1] Masnari, N. A. et al, "Analysis, Design and Fabrication of High Efficiency High Average Power, Pulsed TRAPATT Diode Oscillators," University of Michigan, Electron Physics Laboratory, Final Report HDL-CR-75-201-1, Contract No. DAAG39-74-C-0201, December 1975.

In the work carried out during the present program, the UHF TRAPATT circuit was evaluated in the time and frequency domain as either a lumped or distributed circuit. Voltage and current probes for the S-band and UHF circuits were built and tested. Although the information derived from these studies has given a better understanding of TRAPATT operation, the work has also raised additional questions about the device operation and its interaction with the circuit.

2. UHF Circuit Models

Several computer models were developed to study experimental UHF TRAPATT oscillator units which were received from Harry Diamond Laboratories. These units were developed by Hughes Aircraft Company, Electron Dynamics Division, Torrance, California under ECOM contract DAAB05-73-C-2070. These oscillators were operated experimentally and results similar to the Hughes results were obtained. A typical device generated 250 to 300 W of power in the 700- to 800-MHz frequency range with 25 percent efficiency at 0.1 percent duty cycle.

2.1 Lumped Circuit Model

In an attempt to analyze the performance more thoroughly, several models of the circuit were developed for computer analysis. The first model of the TRAPATT circuit was a lumped element model having the configuration illustrated in figure 1. The element values are as reported in the Hughes Technical Report,[2] which contains

[2]Anderson, L. E., Bowers, H. C., Kramer, N. B., Lane, W. R., Lockyear, W. H., and Obah, C.O.G., "Solid State Microwave Oscillators for Fuses," Final Report No. W-40376, Hughes Aircraft Company, Torrance, CA, May 1976.

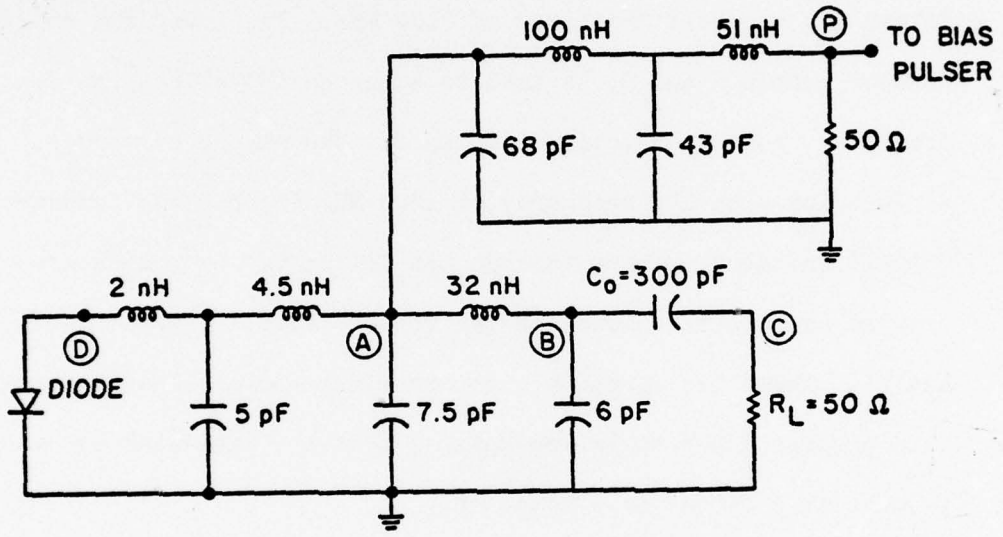

Figure 1. Diagram of 800 MHz lumped element TRAPATT circuit.

a detailed description of the oscillator and its performance. This circuit consists of two low-pass filters connected at point A as illustrated in figure 1. The upper filter (section between points A and P) connects the TRAPATT circuit to the pulser. Its function is to allow a bias pulse to reach the diode but to prevent the TRAPATT signal from leaking back into the pulser. This filter has a cutoff frequency of ~100 MHz. The lower filter (section between points A and C) is used to tune the TRAPATT at the fundamental frequency, but has reactive loading for the higher harmonics. This circuit has a cutoff frequency of 1200 MHz so that the fundamental TRAPATT frequency passes through the filter but harmonics are trapped between the diode and the filter (i.e., between points A and D). These two circuits together limit the oscillator turn-on time This becomes apparent by recognizing that the rise-time-bandwidth product of a filter is a constant,

$$(T_r)(BW) = \text{constant} ,$$

and thus the bias filter, which has a limited bandwidth, will act to limit the rise time of the bias pulse at the diode. For a typical filter the above constant is approximately 0.5, thus resulting in a pulse rise time of approximately 5 ns. Attempts to reduce this rise time by changing the bias-filter structure is counter-productive since it would increase the filter cutoff frequency, thus allowing a portion of the TRAPATT signal to leak back into the bias circuit. In addition, a faster rise time bias-filter configuration would result in the TRAPATT oscillation being affected by any changes in the bias circuit. There is a similar limitation on the TRAPATT RF low-pass circuit. In this case the

cutoff frequency should be approximately 1200 MHz in order to trap the higher-frequency harmonics. For a 1200-MHz cutoff frequency and a $(T_r)(BW)$ constant of 0.5, the minimum rise time for the TRAPATT circuit would be 0.4 ns. As a result of the finite rise times associated with the bias- and RF-filter circuits, if an ideal pulse (zero rise time) were applied at the bias input point (P in figure 1), the low-pass bias-circuit filter would prevent the pulse from appearing at the RF circuit input point (A in figure 1) in a time less than $t \approx 5$ ns. Likewise, the signal would require at least 5.4 ns before arriving at the diode terminals.

To study the rise time of the actual circuit, the time response of the circuit of figure 1 was calculated. The unit-step time response of such a circuit is shown in figure 2. For this case, a unit step was applied at the pulser position and the resulting voltage calculated at the diode and load positions. There are several interesting features in this figure. First, the finite rise time is approximately 5 to 10 ns, which is in agreement with that predicted by the simple calculation. Second, there is an overshoot of the bias pulse, with the maximum voltage across the diode position approximately 1.35 times as large as the steady-state value. Third, there is a circuit oscillation with a frequency of 140 MHz that slowly dies out as the circuit reaches steady state. For the 200-ns-wide pulses used in these experiments, this oscillation occupies 25 percent of the total pulse time.

The results illustrated in figure 2 were for the case where the diode was considered as a 50-Ω impedance. Figure 3 compares three cases in which the diode impedance takes on values of 50, 100, and 1000 Ω, respectively. Note that the effect of the

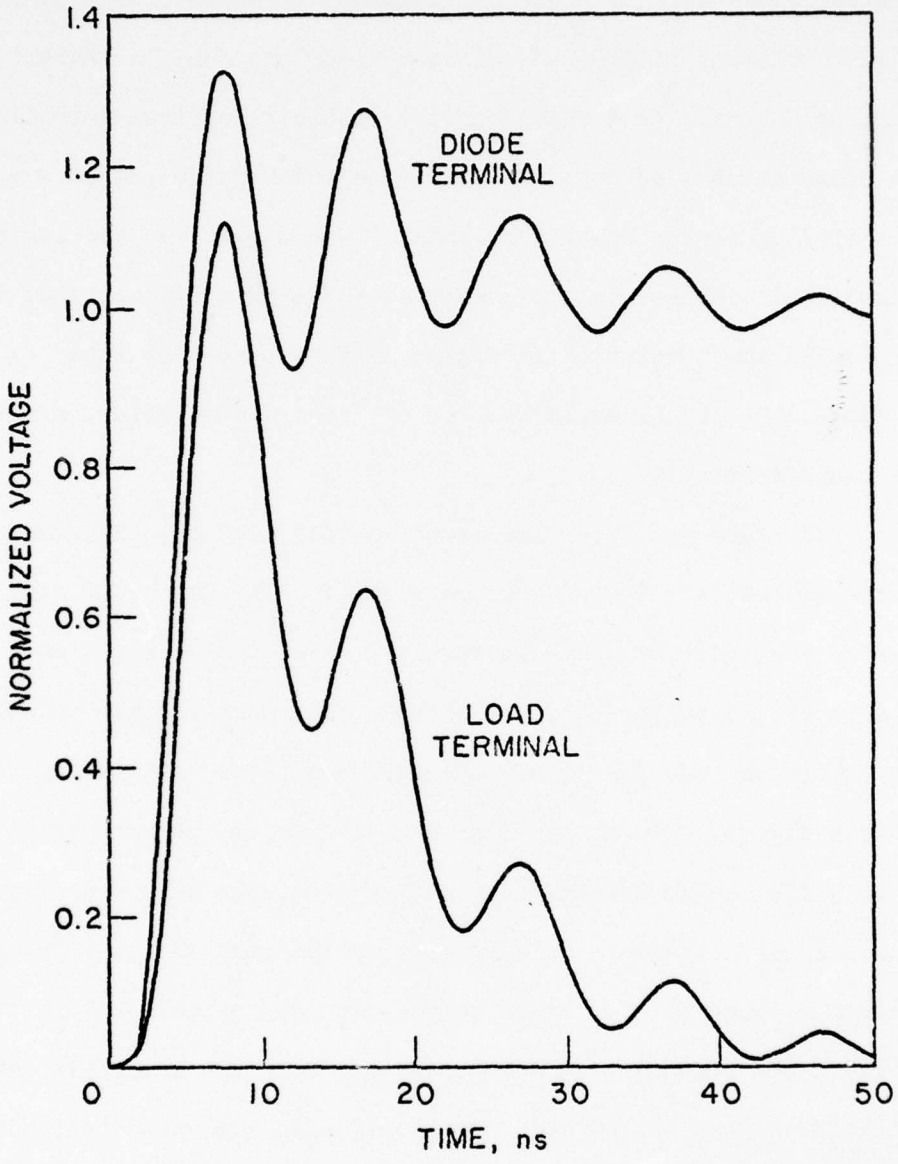

Figure 2. TRAPATT circuit step response as observed across the diode and at the load terminals.

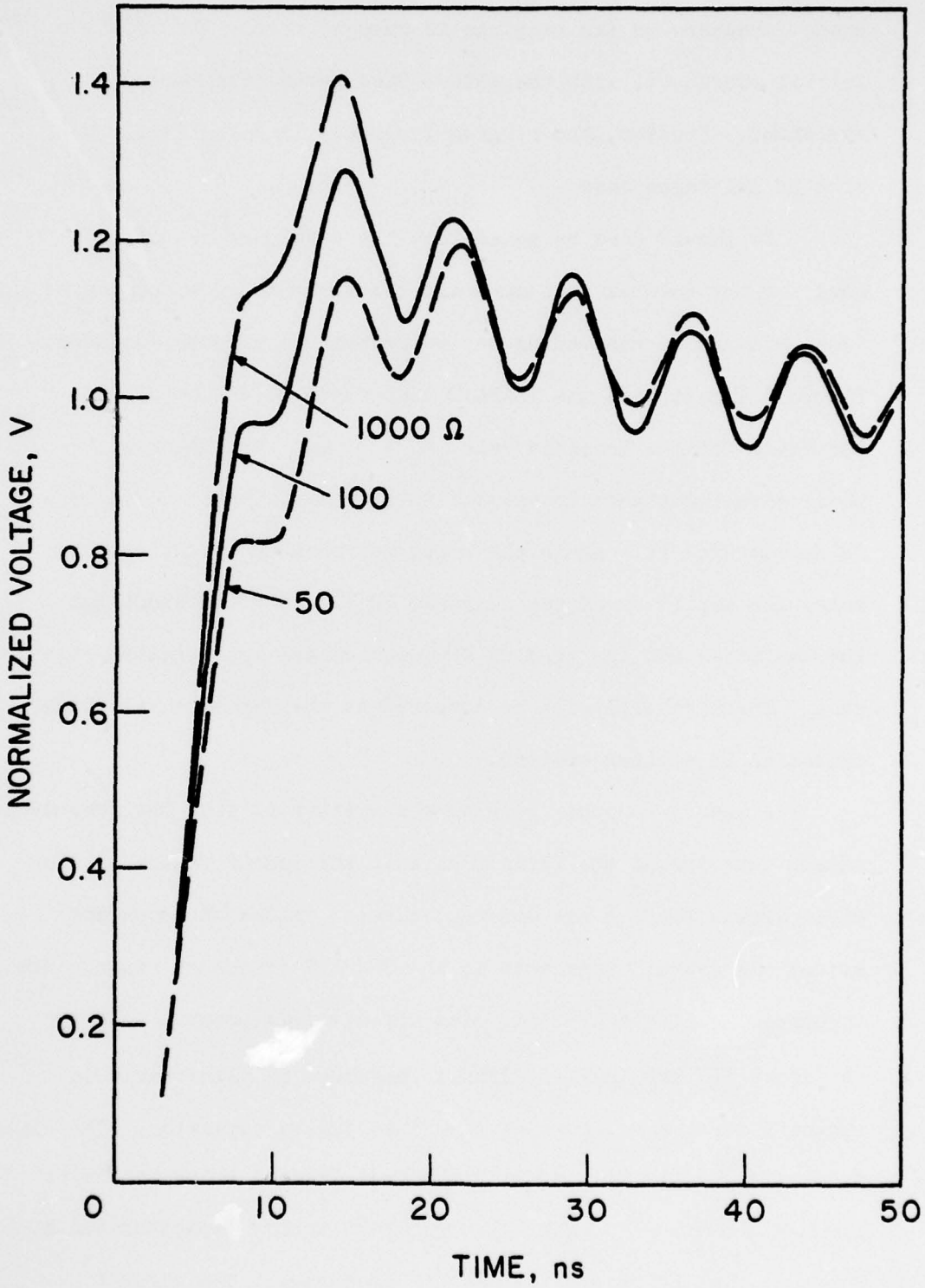

Figure 3. Effect of diode impedance on the TRAPATT circuit response as observed across the diode terminals.

diode impedance on the response is only to change the amount of initial overshoot, with the 1000-Ω case having the largest overshoot. However, the ringing frequency is essentially the same in all three cases.

It should also be noted that the preceding results were for the special case where all the elements were considered ideal with no corresponding series resistance effects included. Figure 4 illustrates the TRAPATT step response at the diode terminals for the lossless case ($R_S = 0$) and for the case where each inductance is assumed to have a resistance of $R_S = 1\ \Omega$ in series with it. Again the basic response is essentially the same; the amplitude of the response is slightly different for the two cases, but the ringing frequencies are approximately the same. These results will be compared to the experimental diode operation in a later section.

A second computer program was written to find the frequency domain behavior of the TRAPATT circuit portion of figure 1. The bias-circuit portion has constant element values and does not affect the overall impedance in the TRAPATT frequency range. The impedance looking toward the bias circuit from point A is shown in figure 5. The TRAPATT circuit impedance is illustrated in figure 6 for three values of the first tuning capacitor. The circuit acts as a low-pass filter with the real loading being small for frequencies above 500 MHz. Changing the tuning capacitor value does not greatly change the cutoff frequency. The circuit is resonant at 200 to 400 MHz, depending on the value of the tuning capacitor. At frequencies higher than several

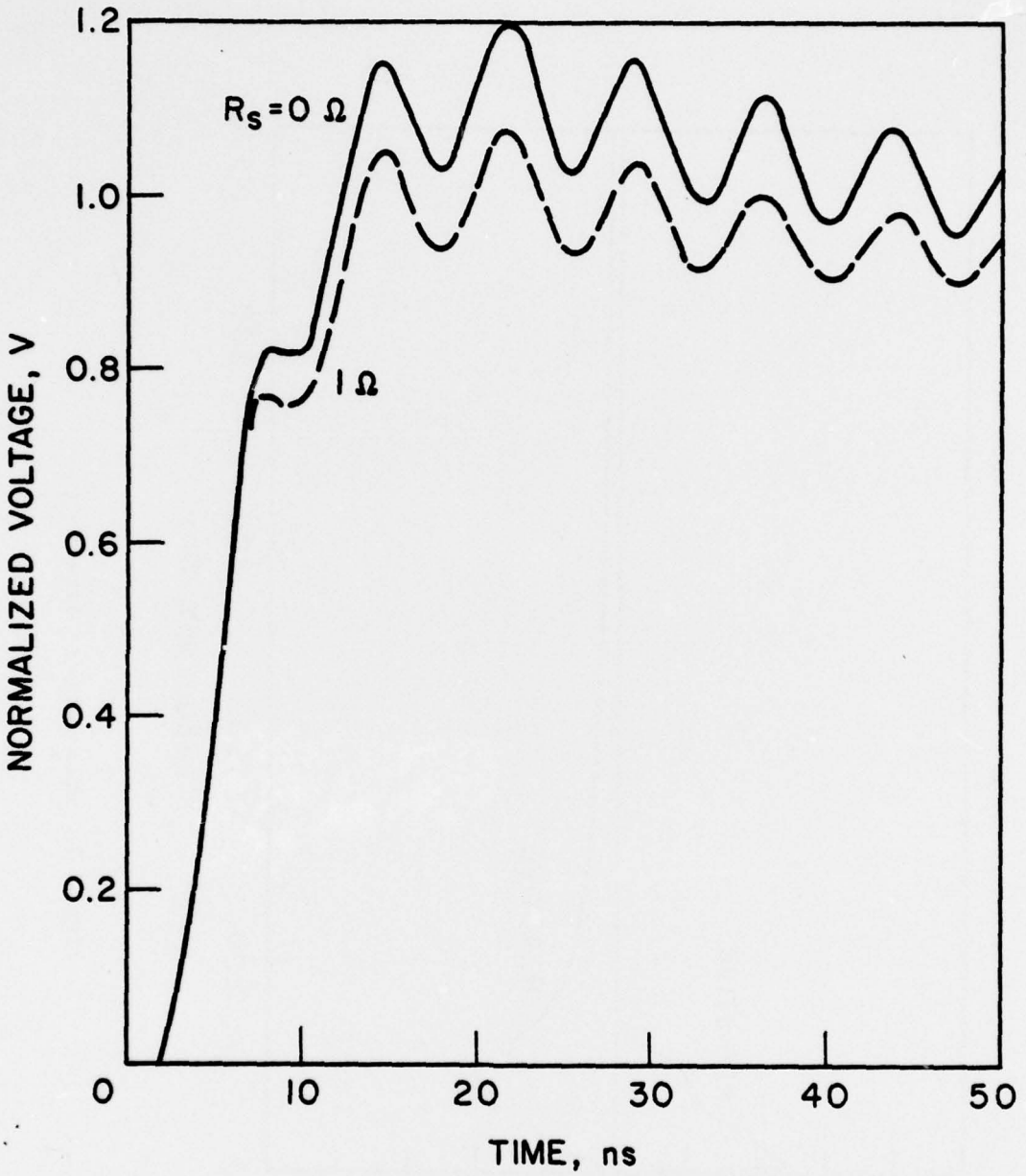

Figure 4. Effect of finite resistance values in series with the inductors on the TRAPATT response at the diode terminals.

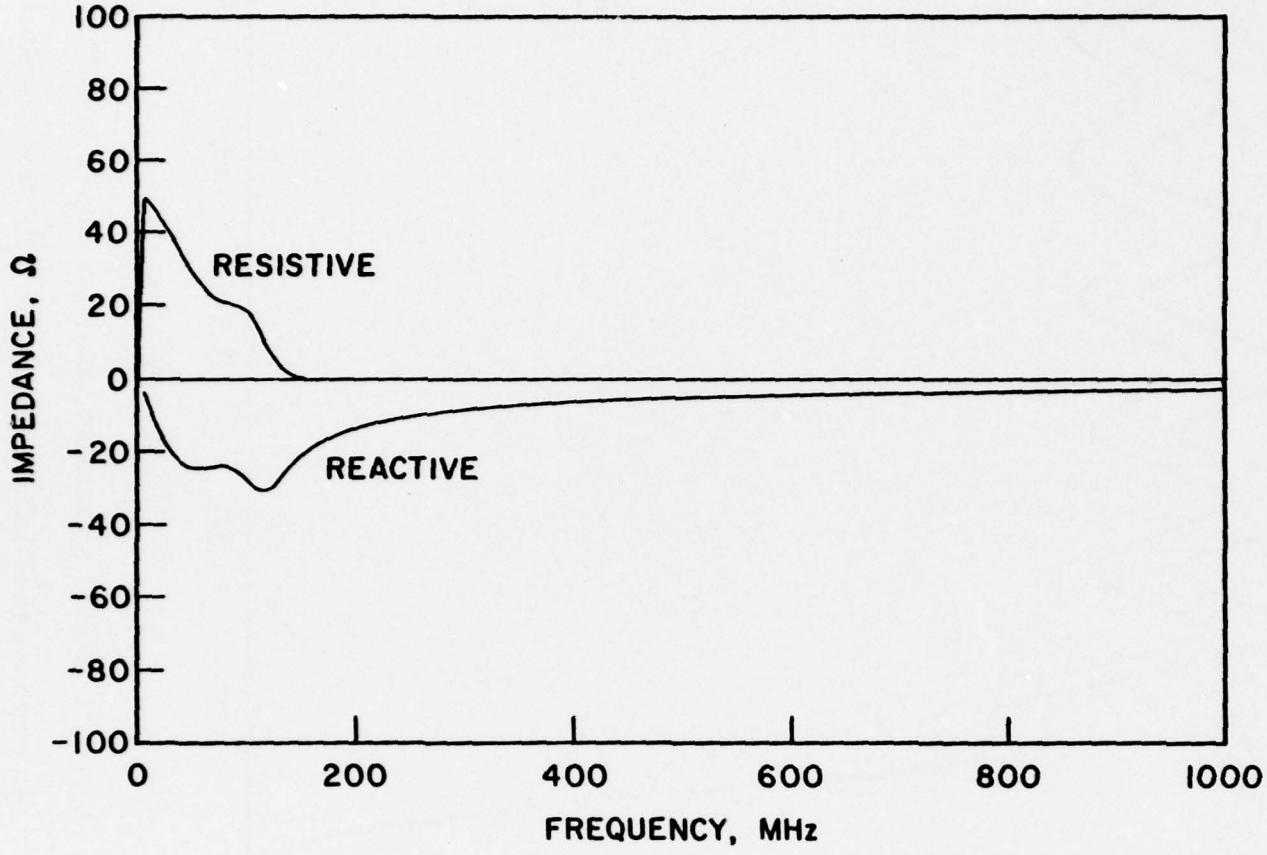

Figure 5. Bias circuit impedance.

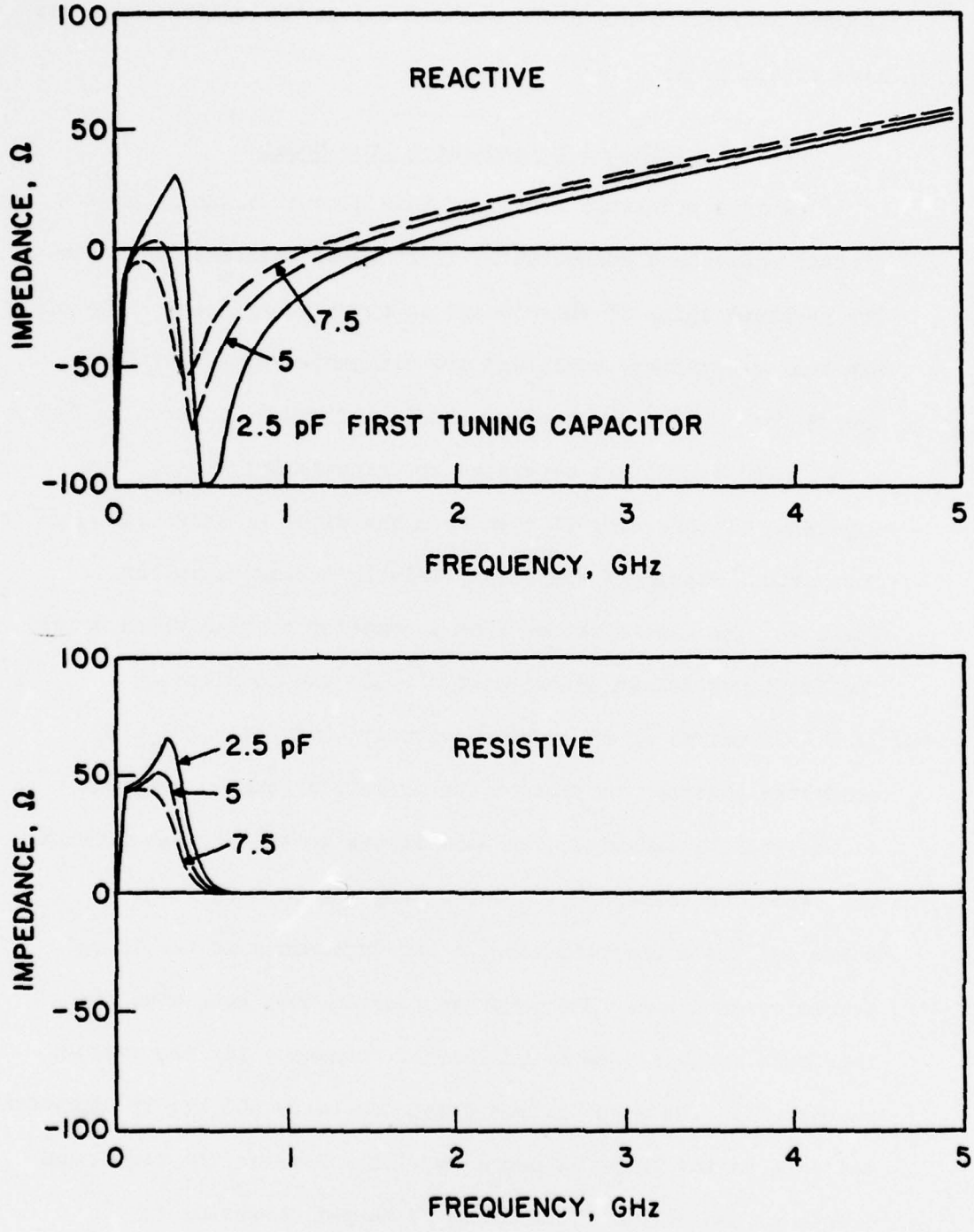

Figure 6. Lumped element TRAPATT circuit.

GHz the reactance is dominated by the 2-nh series inductor located nearest to the diode, and changes in the tuning capacitor have little or no effect.

2.2 Distributed Transmission Line Model

A more realistic model for this circuit assumes lumped-circuit capacitors connected by distributed transmission lines. The physical shape of the circuit is shown in figure 7. The diode and tuning-capacitor positions are designated with + symbols in the figure. The corresponding electrical model is shown in figure 8 with lumped capacitors separated by transmission lines. The impedance of this circuit seen from the diode is shown in figure 9 for various values of the first variable tuning capacitor. These results were obtained from a computer program which models the frequency domain distributed circuit and operates on the [A B C D] matrix of the various circuit elements which are connected together to produce the overall frequency response of the TRAPATT circuit. The data inputs to the program include the capacitor values (C_1, C_2, C_3, C_B), the 50-Ω resistor value, and the electrical lengths and impedances of the three transmission lines. The computer program then generates the impedance variation as a function of frequency for the various parameters. The value of the impedance below 500 MHz is approximately the same as the lumped element version. However, the electrical length of the circuit from diode to output connector is approximately 10 cm. For frequencies higher than 500 MHz the distributed nature of the circuit changes the impedance presented to the diode. The three curves in the plot indicate that changing

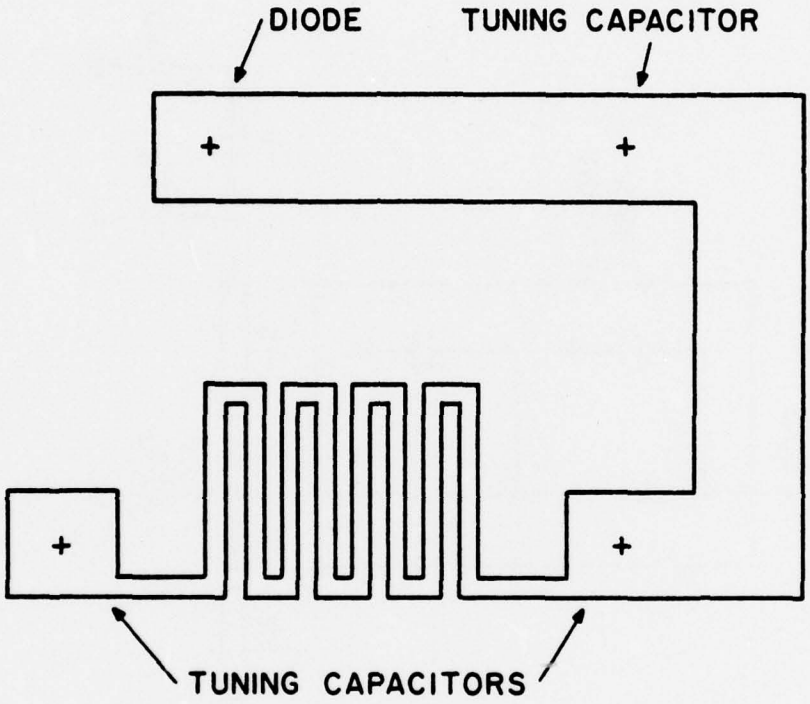

Figure 7. Physical layout of 800-MHz oscillator.

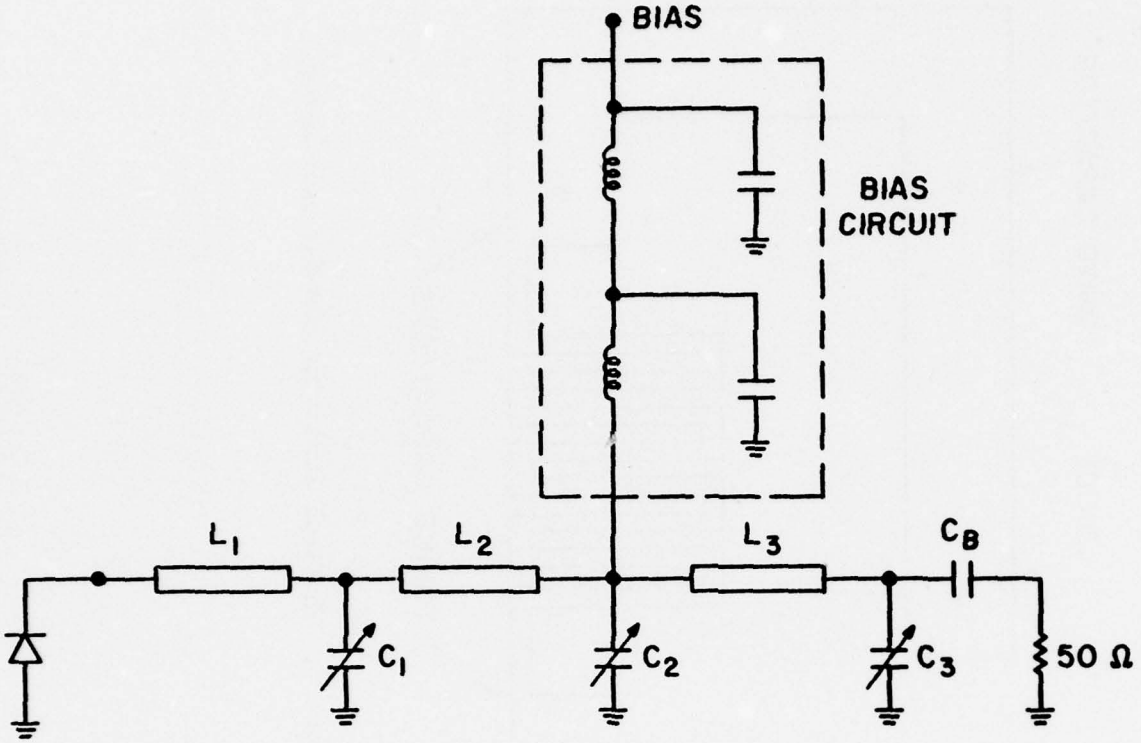

Figure 8. Equivalent circuit.

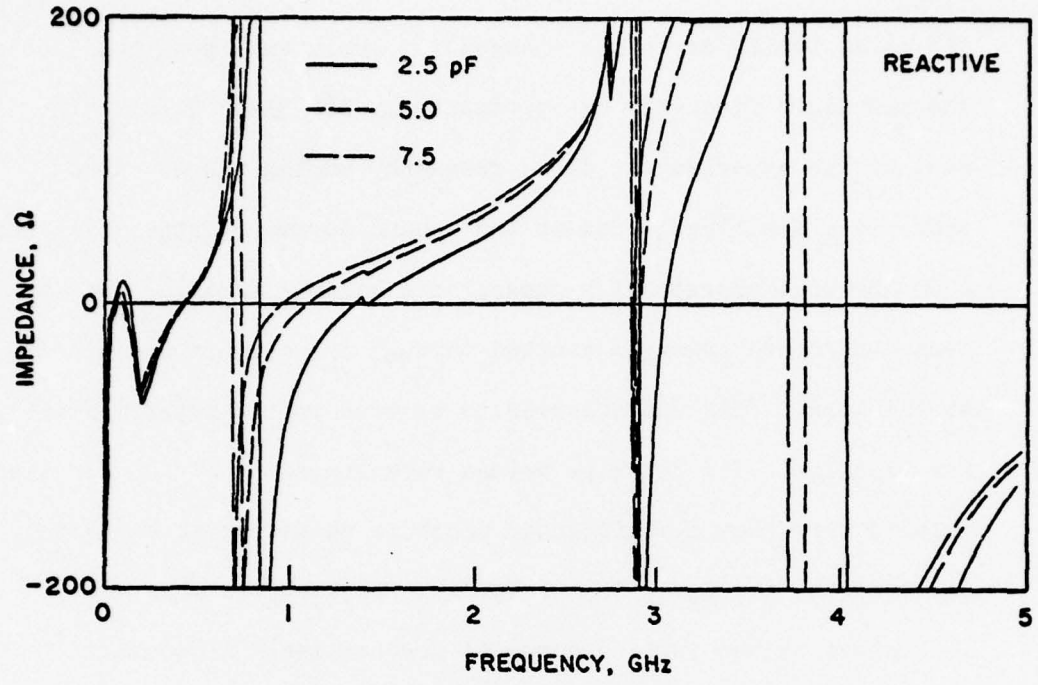

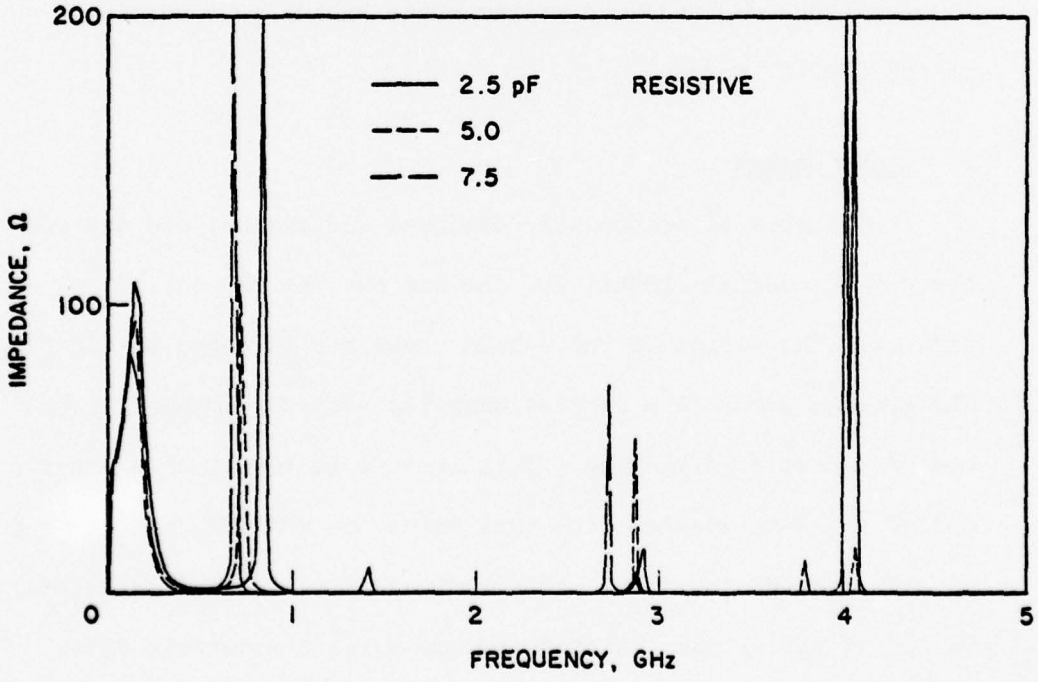

Figure 9. Distributed circuit impedance.

the first tuning capacitor changes the resistance peak position and the resonance frequency by approximately 100 MHz. This is the same as the experimental diode frequency tuning range. Also, there is a small real load at the second harmonic frequency around 1500 MHz that changes with capacitance value. Thus, some of the second harmonic power is coupled through the circuit and appears at the load. This was observed to be true in the experimental results also. The reactive values were limited to ± 200 Ω. These results show that a distributed model is necessary to accurately describe the impedance of the TRAPATT frequency as well as the impedances of the various harmonic frequencies. Although it has not been implemented the next step would be to couple a diode simulation program to the circuit model to study the transient response and steady-state operating conditions of the TRAPATT mode.

3. Probe Design

Two sets of probes were designed and tested, one set for the S-band coaxial circuit and one set for the UHF stripline circuit. The design of the S-band probe set is shown in figure 10. The present probe is a current sampling resistor mounted in the end of a 3-mm coaxial line. This line is in turn mounted at the end of the 7-mm coaxial line that forms the TRAPATT cavity. The current through the diode is determined by measuring the voltage developed across the resistor through which the current flows. This signal is transmitted by a coaxial line to the recording oscilloscope. The first voltage probe used was a carbon-coated ceramic cylinder placed around the diode package. The resistance of the

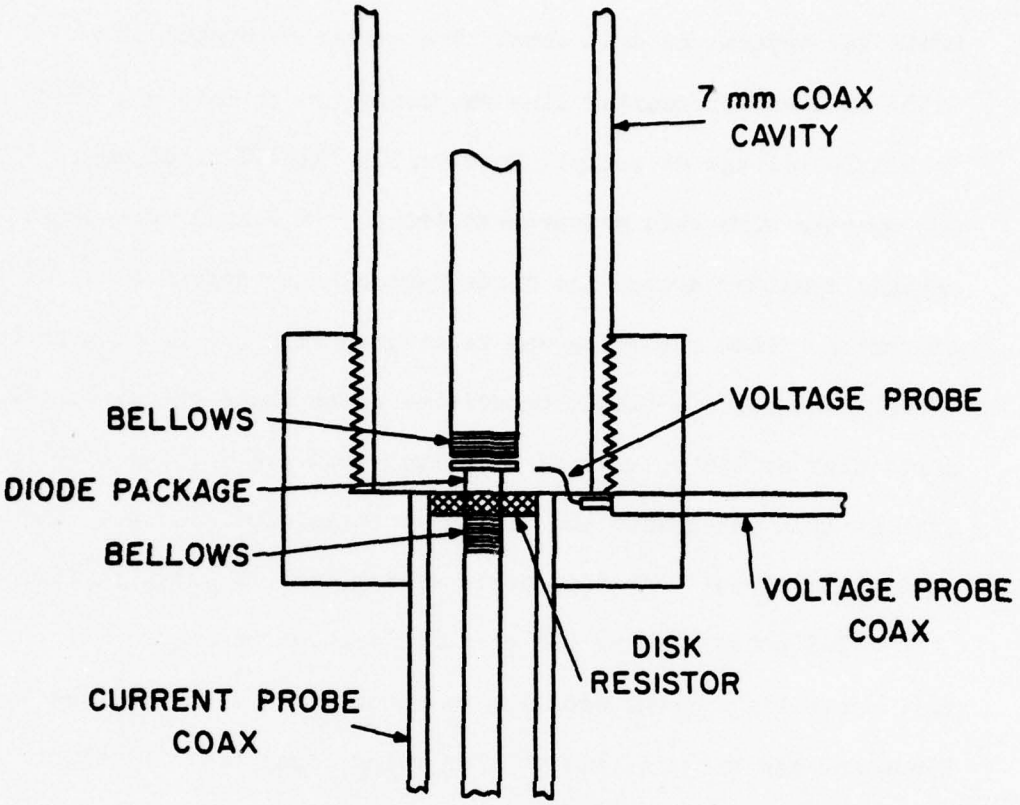

(a) Probe layout

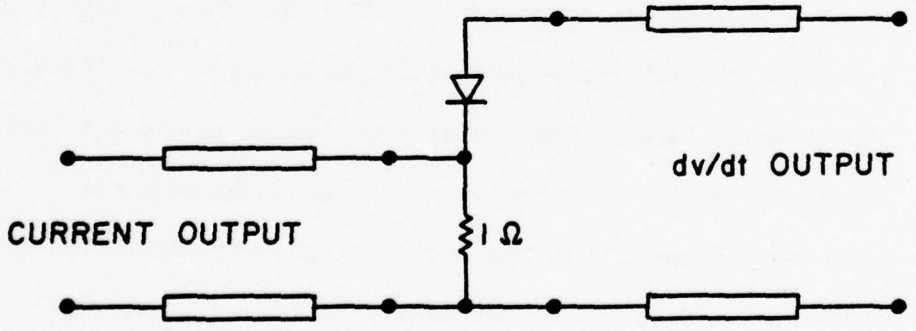

(b) Equivalent circuit

Figure 10. S-band probe set design.

probe was several hundred ohms. The center conductor of a 0.086 cm diameter coaxial line was connected to this cylinder to sample voltage directly. However, the TRAPATT diode would not operate with this measurement setup. A simple non-coated ceramic cylinder around the diode package also degraded the diode operation. Thus, the probe was redesigned with the present probe arrangement being a simple capacitive probe whose output is the derivative of the voltage dV/dt rather than the voltage itself. This is then integrated and displayed on an oscilloscope. The equivalent circuit for this probe arrangement is shown in figure 10b.

The probe for the UHF circuit is shown in figure 11. In this probe the current-sampling resistor was mounted between the diode and the circuit, rather than being connected directly to ground as in the S-band design. The probe was designed in this way since mounting the resistor below the diode would greatly increase the thermal resistance. Because of the large dc powers involved in the operation of the UHF device, it was felt that the increased thermal resistance would result in the destruction of the diodes. Because the resistor was above ground two leads were necessary to allow the resistor voltage to be measured. Two coaxial leads were connected to the oscilloscope which was operated in a differential mode for determination of the current. The voltage probe for the VHF circuit was a Tektronix P6056 oscilloscope probe. The equivalent circuit for this probe arrangement is shown in figure 11b.

Several problems have occurred in the operation of these probes. The main problem was inherent in the nature of the sampling

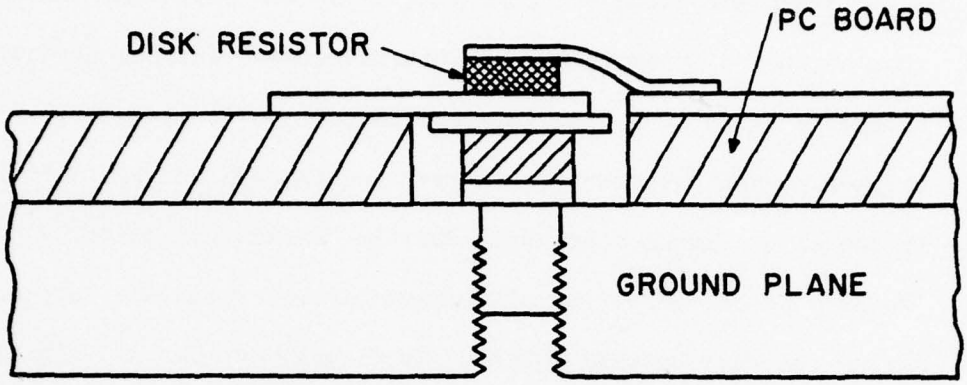

(a) Probe layout

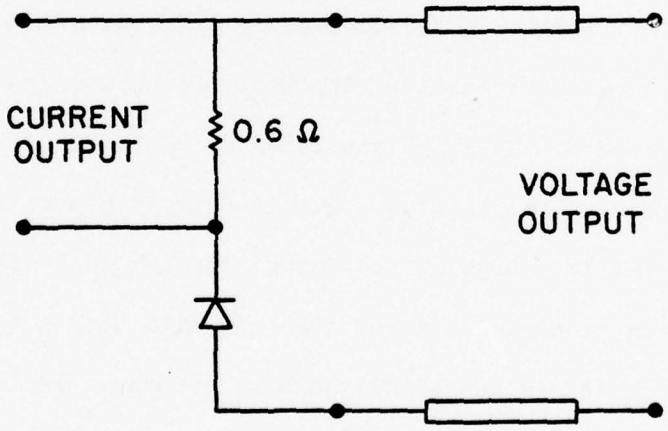

(b) Probe equivalent circuit

Figure 11. Schematic diagrams of probe for UHF circuit.

oscilloscopes that were used. Sampling oscilloscopes are designed to display a repeating signal by sampling at small Δt time intervals after a zero-crossing or triggering event has occurred. The time between samples is several microseconds. The high-frequency trigger circuit is a blocking-oscillator-type design where the trigger circuit operates in a free-running mode and is locked to the input signal. However, for the TRAPATT oscillator with low duty cycle, this type of trigger circuit primarily samples during the time between pulses. To display the TRAPATT signal, the oscilloscope must sample only during the on-time of the oscillator. This requires the use of the lower-frequency Schmitt trigger type of triggering. Since this trigger mode is designed for low-frequency operation, it must be very carefully adjusted for TRAPATT operation. A second type of triggering is used to display the rise time and transient response. In this case the oscilloscope is triggered by the pulse generator which is used to bias the oscillator. Since this is a stable trigger signal the display is also stable. However, the actual TRAPATT oscillation has a starting jitter and is not coherent with the pulser trigger signal, so it can not be displayed. However, the low frequencies and IMPATT oscillations that trigger the diode are easily detected.

4. UHF Diode Turn-On Conditions

Previous work in this program has shown that the S-band coaxial-circuit TRAPATT mode could be triggered by either an IMPATT-mode oscillation, a VHF bias-circuit oscillation, or a combination of the two. Similar results have been found for the

UHF devices. The time between pulses also affected the turn-on conditions.

The IMPATT mode of operation, which occurs prior to the TRAPATT, is observed under the proper biasing conditions. The IMPATT mode occurs under relatively slow turn-on conditions. This can be explained by referring to the theory of IMPATT operation. Assuming that the circuit is tuned correctly, the IMPATT mode will exist over a range of currents. At low currents, the device negative resistance is matched by diode and circuit losses. As the current increases, the negative resistance improves and the IMPATT oscillation starts. At large-current levels, nonlinear and space-charge effects within the diode degrade the negative resistance and the diode eventually ceases to oscillate. The time required for the IMPATT oscillations to build up depends on the difference between the device and circuit resistance. For a relatively slow risetime pulse, the time spent in the potential IMPATT mode range is longer than the IMPATT mode build-up time, thus resulting in the generation of the IMPATT mode. For a fast rise-time pulse, the current goes through this range before the IMPATT mode can build up and thus it never comes into existence. There are, however, other types of triggering that occur under fast rise-time pulse operation. Since the starting of the TRAPATT mode as initiated by the IMPATT mode triggering typically requires longer time, changing the shape of the pulse will change the turn-on time, the turn-on mechanism, and will possibly also affect the pulse-front jitter. For the purpose of these discussions, the turn-on time is defined as the period from the time the voltage

first reacnes the breakdown voltage until the start of oscillation. The various types of mechanisms that can trigger the TRAPATT mode are illustrated, beginning with figure 12. This figure shows a slow rise time pulse with the resulting IMPATT mode turn-on. The breakup at the leading edge of the pulse will be discussed below. There is a period of approximately 20 ns during which the IMPATT oscillation is present. This is illustrated in the middle portion of the photo. An enlarged view of the IMPATT oscillation is shown in figure 13. This photo shows a portion of the 5-GHz IMPATT oscillation, which also appears in the middle of figure 12. The frequency changes from approximately 4 to 5 GHz, depending on the drive current level, with constant circuit tuning. This is the same as the frequency tuning dependence with $\sqrt{I_{DC}}$ in IMPATT oscillators. Figure 14 shows the transition from IMPATT to TRAPATT oscillation. The left part of the figure shows the IMPATT oscillation of figure 13, and the right part is the TRAPATT frequency oscillation. The middle section denotes the transition time of approximately 4 ns consisting, in sequence, of a 1-ns wave, a 2-ns (approx) sine wave, and another 1-ns wave, all growing in amplitude with time. The TRAPATT oscillation starts 3 ns from the right edge of the photo.

A non-IMPATT startup is shown in figure 15. In this case the rise time is fast enough to prevent IMPATT buildup. Figure 16 shows the start of the TRAPATT oscillation at the top of the pulse in figure 15. Figure 17 is an expanded version of figure 16. The high-frequency oscillation is absent from this photo; the TRAPATT oscillation begins approximately 5 ns from the right edge

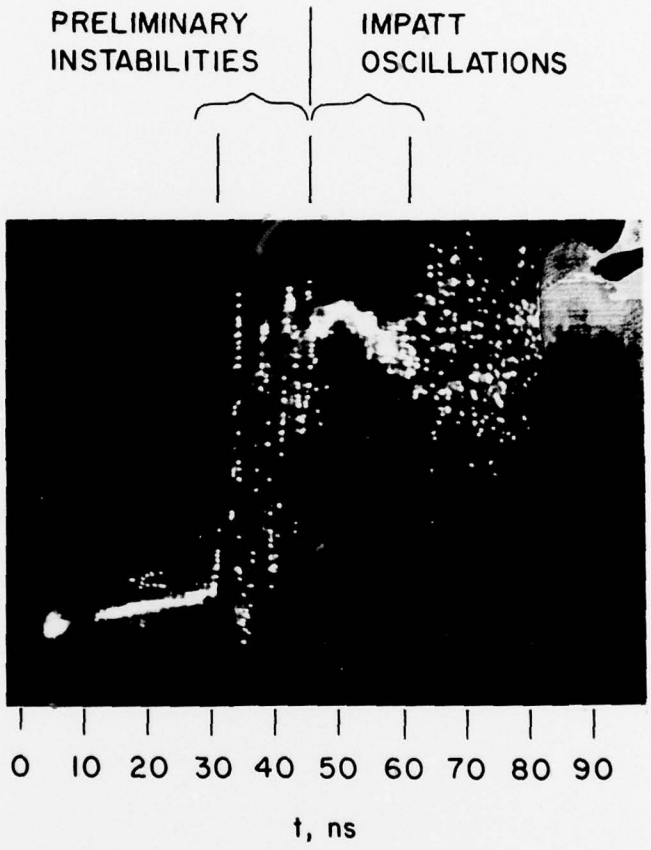

Figure 12. Signal detected at the diode for a slow rise-time moderate amplitude bias pulse (10 ns/div).

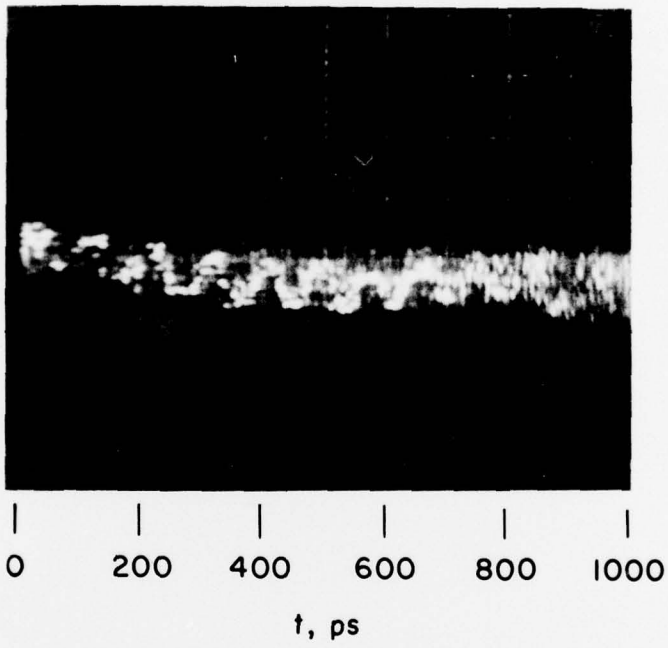

Figure 13. Signal detected at the diode illustrating the presence of the IMPATT frequency at approximately 5 GHz (200 ps/div).

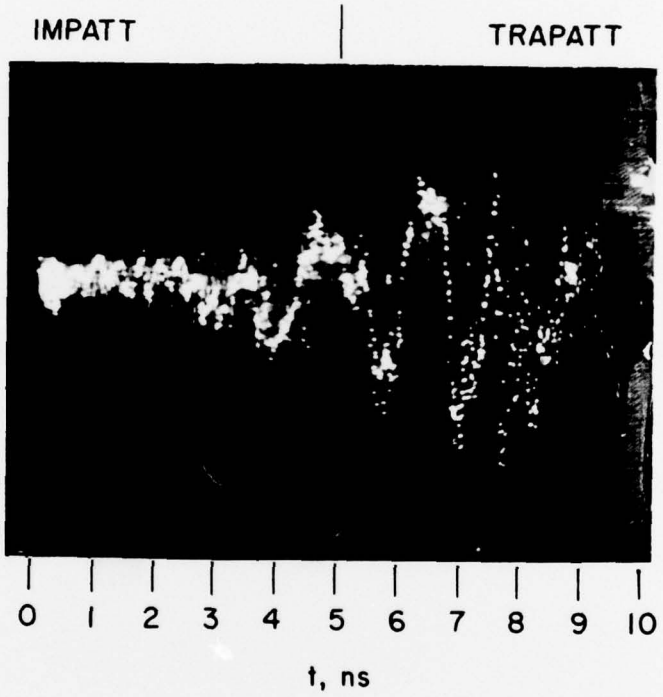

Figure 14. Signal at the diode illustrating the transition from the IMPATT mode to the TRAPATT oscillations (1 ns/div).

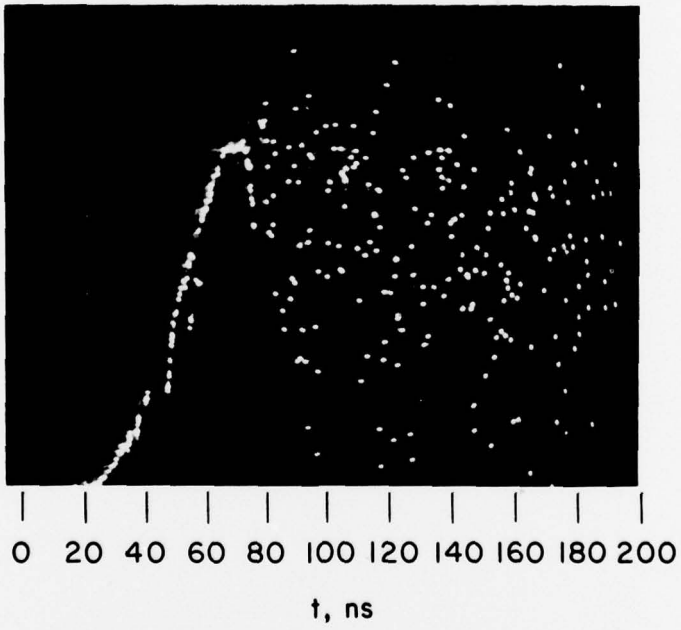

Figure 15. Signal at the diode when a large amplitude, fast rise-time bias pulse is applied (20 ns/div).

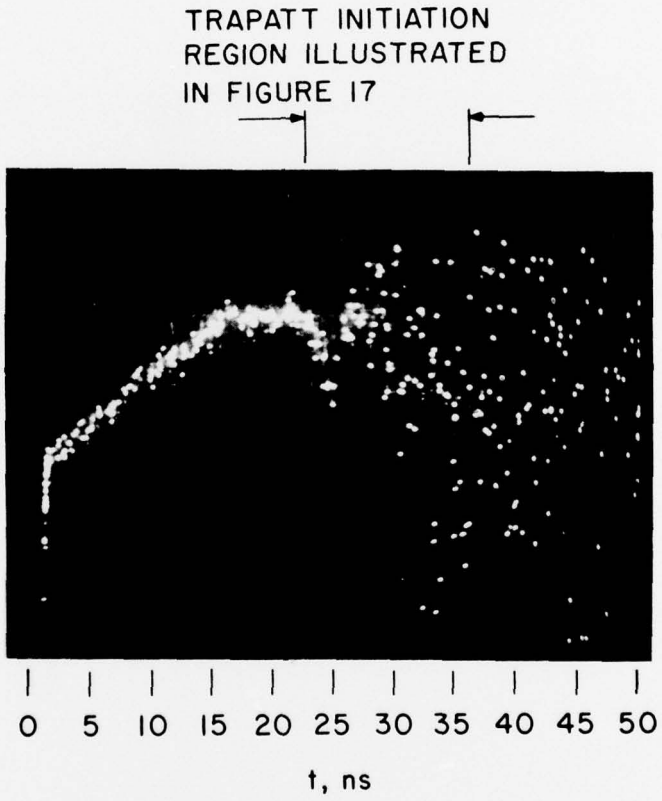

Figure 16. Signal at the diode illustrating the direct transition to the VHF oscillations with no intervening IMPATT signal (5 ns/div).

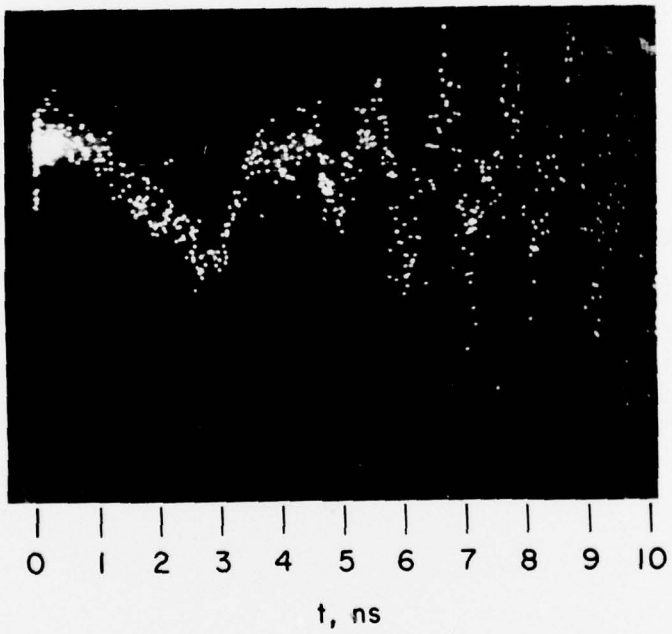

Figure 17. Signal at the diode illustrating the beginning of the TRAPATT mode (1 ns/div).

of the photo, following a 2-ns transition region from the rising pulse.

The shape of the bias pulse was also found to depend on the time between the pulses. Pulse spacings less than 40 to 50 ns give a ringing on the leading edge of the bias pulse, such as that illustrated in figure 12. Initially, this was thought to be indicative of higher harmonics of the TRAPATT frequency being trapped in the circuit between the diode and the low-pass filter. Based on the computer model of figure 9, these higher harmonics are found to be very lightly loaded. If the power decays in a time longer than the time between pulses, this power could distort the start of the pulse. This would also explain the turn-on jitter, since the turn-on time of the oscillator depends on the initial state of the diode. However, the signal across the diode is observed to decay in 30 to 50 ns, thus eliminating the above as a potential jitter-causing mechanism. The rapid decay of trapped harmonics was measured by using a sampler with an appropriate PIN switch. The voltage across the diode was gated into an oscilloscope at various times before and after the TRAPATT pulse. The PIN switch was biased with a variable time-delay pulse generator that was also used to trigger the main high-power diode pulser. A more plausible explanation for the startup jitter would be in the inherent differences which exist between successive pulses. However, the experimental results obtained in this program are not definitive enough to establish any single mechanism as the predominant jitter-causing effect.

The voltage probe was also used to measure the presence of the TRAPATT harmonics at the diode. This was done by passing the signal from the voltage probe through a tunable YIG filter and reading the output power with a power meter. The diode was operating at 750 MHz with a peak power output of 250 W and a 0.1-percent duty cycle. Table I shows the resulting signals with the power at each frequency being normalized to the second-harmonic power.

The power at the 750-MHz fundamental frequency cannot be measured here since the frequency is below the minimum frequency of the YIG filter. The many signals that are present clearly demonstrate the importance of the distributed-circuit model discussed above. It should also be noted that there is a large amount of power in the higher harmonics, with the 6th harmonic having the highest power of all. This shows the importance of designing TRAPATT oscillator circuits based on consideration of a large number of frequencies. Unfortunately, this makes the problem of circuit design much more difficult.

5. Conclusions and Suggestions for Further Study

Work carried out during this program has resulted in circuit models of the UHF TRAPATT circuit for both lumped and distributed cases. Since the TRAPATT circuit supports many higher harmonics, the distributed circuit must be considered in order to accurately model the operation. The diode turn-on conditions have been measured and found to be similar to those of the S-band devices studied. In particular, the experimental

Table I. Signals detected during TRAPATT operation.

Frequency (MHz)	Harmonic	Relative Power
1490	2 f_o	1
2220	3 f_o	1.11
2950	4 f_o	0.49
3730	5 f_o	1.85
4470	6 f_o	3.02
4860	IMPATT	0.28
5250	7 f_o	0.47
5950	8 f_o	0.79
6420	≈ 9 f_o	0.82
7390	10 f_o	0.58
8184	11 f_o	0.22
9000	12 f_o	0.46
9290	≈ IMPATT + 6 f_o	0.24
9620	13 f_o	0.49
10,370	?	0.15

results clearly indicate that the appearance of the TRAPATT frequency is always preceded by VHF oscillations which are characteristic of the RF circuit. The IMPATT signal, on the other hand, will only occur if the bias-pulse rise time is slow and its amplitude moderate. Thus, the TRAPATT turn-on characteristics are dependent on both the bias circuit (bias pulse shape characteristics) and the RF circuit (VHF oscillation characteristics). The triggering mode could be switched by changing the bias-circuit conditions. The turn-on time can be minimized (10 ns or less) by applying a fast rise-time bias pulse having substantial overshoot (e.g., 20 percent overshoot). The absolute minimum turn-on time has not been determined but obviously cannot be shorter than the build-up time associated with the establishment of the trapped plasma.

In summary, it can be stated that:

(1) The TRAPATT is capable of stable high-power pulsed operation, provided the device and circuit are properly matched.

(2) The TRAPATT turn-on time is related to the RF and bias-circuit characteristics.

(3) The jitter associated with the turn-on is inherent in the basic characteristics of the TRAPATT and its associated circuit.

At this point an improved understanding has been obtained of the TRAPATT physical behavior as well as its interaction with the circuit. It is apparent that the device is critically dependent on the circuit for its operation. Devices having different characteristics (doping profiles, etc.) will behave similarly

when placed in the same circuit. However, there are some important questions that need to be resolved before a complete understanding can be obtained.

Additional work is needed on refining the current and voltage probing techniques so that accurate wave shapes can be obtained. These could then be Fourier analyzed to determine the diode impedance at the TRAPATT and its harmonic frequencies. This information could be coupled with the distributed circuit models that have been developed so that the device-circuit interaction could be properly modeled and thoroughly studied. In addition to optimizing the circuit for TRAPATT operation, the technique should also be useful in allowing a comprehensive analysis of the transient behavior of the diode to be obtained. Furthermore, a transient analysis has been developed on an Army Research Office sponsored project entitled "Fundamental Problems in TRAPATT Oscillators and Amplifiers." This analysis has direct application to the types of problems that we are considering here. The turn-on conditions could be thoroughly studied and the jitter problem could be evaluated starting from the realistic model. Presumably, the analysis would identify the basic mechanisms responsible for the turn-on jitter, thus making it possible to reduce the jitter to the lowest possible level and improving the operation of the device.

The distributed circuit model when used in conjunction with a realistic device model should also help in the design of optimized TRAPATT oscillators and amplifiers. Finally, the intermodulation effects should be evaluated. As described

in the report, in addition to the fundamental TRAPATT frequency there are also other signals present in the vicinity of the diode. These include harmonics of the TRAPATT frequency, bias circuit oscillations, VHF oscillations and IMPATT oscillations. These signals may interact with each other, so that all intermodulation products that fall within the pass-band of the RF circuit will be transmitted to the load along with the TRAPATT fundamental.

Only with a thorough understanding of the above areas will it be possible to have sufficient knowledge of the TRAPATT operation to allow optimized devices and circuits to be designed.